Journal of Materials Chemistry

Cite this: *J. Mater. Chem.*, 2011, **21**, 17033

www.rsc.org/materials

HIGHLIGHT

How to exploit the full potential of the dip-coating process to better control film formation

David Grosso*

DOI: 10.1039/c1jm12837j

Dip-coating is an ideal method to prepare thin layers from chemical solutions since it is a low-cost and waste-free process that is easy to scale up and offers a good control on thickness. For such reasons, it is becoming more and more popular not only in research and development laboratories, but also in industrial production, as testified by the increasing number of annual publications (9, 180, and 480 articles in 1990, 2000, and 2010, respectively). Even so, the full potential of dip-coating has not yet been fully explored and exploited. This article highlights the recent progresses made by tuning the processing conditions beyond conventional ranges to prepare more and more complex and controlled nanostructured layers. Especially, we will see how one can take advantage of an accurate tuning of the withdrawal speed and of the atmosphere to control the nanostructuration originating from evaporation-induced-self-assembly (EISA), together with the final thickness from a few nm up to 1 μm from the same initial solution. A new regime of deposition, involving capillary induced convective coating that is highly suitable for the deposition from aqueous and/or highly diluted solutions, will be described. Finally, it will be demonstrated that dip-coating is also a well suited method to impregnate porosity, to make nanocomposites, or to perform nanocasting. The present discussion is illustrated with systems of interests in domains such as optics, energies, nanoelectronics, nanofluidics, *etc.*

Introduction

Thin films are extremely important systems that are used in many domains of application since they bring an additional function at the surface of any kind of materials. The preparation of coatings is achieved either by a dry process (CVD, PVD, PECVD, *etc.*) or by a wet process (spray coating, brush casting, spin coating, dip coating, *etc.*), also addressed as Chemical Solution Deposition (CSD). These wet methods are well adapted for the preparation of multi-phase materials since any non-volatile compound that is dispersed or dissolved into the solution will be homogeneously distributed or organised into the final films, and with a fairly good control of the thickness.[1] For instance hybrid organic/inorganic, or composite, layers are easily obtained by evaporation of solutions containing metal oxide precursors, organic functions, monomers, polymers or various kinds of nanoparticles. It is also highly appropriate for the preparation of materials with controlled porosity since porogenic species can easily be embedded and eliminated from the final material. For

Chimie de la Matière Condensée de Paris, UMR UPMC-CNRS 7574, Université Pierre et Marie Curie (Paris 6), Collège de France, 11 place Marcelin Berthelot, 75231, Paris, France. E-mail: david.grosso@upmc.fr

David Grosso

Prof. D. Grosso was appointed as associate professor in 2002, and as full-professor in 2007, at the University of Paris. He works in the Laboratory Chimie de la Matière Condensée de Paris (LCMCP) on processing nanostructured materials through bottom-up approaches. He is a co-author of more than 120 articles and 10 patents. His work was awarded by the International Sol–gel Society (ISGS) in 2005 and by the French Society of Chemistry (SFC) in 2009. He is a junior member of the French Institute of University since 2009, and he is a co-founder of a start-up "Pomatec" developing chemical surface treatment for stones.

instance, metal oxide[2] and polymer[3,4] coatings with extremely well ordered nanopores were prepared using the Evaporation-Induced-Self-Assembly method.[5]

Among the various methods available to perform liquid deposition, dip-coating has always been the most attractive one because of its simplicity and easiness to operate, and because no solution is wasted and it offers a relatively fair control over the thickness. However some drawbacks are associated to this technique. First, one faces the difficulty to homogeneously wet the substrate, especially when high surface tension solvents, such as water, are used. The thickness becomes difficult to control when ultra-thin (<20 nm) or ultra-thick (>1000 nm) layers need to be prepared from highly diluted or highly viscous solutions. Another challenge concerns the deposition onto porous substrates, or onto porous layers, such as in the case of multilayer systems involving ITO, FTO, or sputtered Au for instance, within which the solubilised precursors may infiltrate and modify their initial properties. Another important obstacle common to all CSD methods resides in the formation of cracks often resulting from the presence of lateral tensile stress occurring during drying, and/or consolidation.[6,7] This is especially encountered for thick and hard ceramic layers, for which the adhesion force to the substrate may not be sufficient to overcome the lateral tensile stresses. Even if this technique is commonly used in R&D laboratories and industries in various fields of applications, not much effort has been dedicated to solve the latter problems or even to better understand the involved physical–chemical phenomena so as to exploit further the potential of this simple process.

Here, we report on the most recent progresses made in the control of the dip-coating process and how they can partly solve the latter associated drawbacks. The discussion is based on a recent innovative study of the variation of film thickness and quality with respect to the withdrawal speed and to the atmosphere of evaporation. A simple semi-experimental model, describing the whole relation linking the chemical and the processing conditions to the final film thickness, is reported.[8] The latter model has been verified for dense, porous, polymeric, ceramic and composite films. The following behaviours that contrast with what is usually admitted are addressed.

- The thickness does not always increase when the withdrawal speed increases, since a reverse tendency is observed in an additional regime of deposition taking place at ultra-low withdrawal speed, where evaporation and capillary convective effects govern the deposition rate.

- Any aqueous solution can easily be deposited when proper processing conditions are applied.

- Ultra-thick and ultra-thin films can be prepared directly from the same initial, highly diluted or highly concentrated, precursor solution (aqueous or organic media).

- Porosity of the substrate, or of the underlying layer, is not always a problem and can either be eluded or properly utilised, especially in nanocasting procedures.

- The critical thickness for which crack formation occurs can be considerably increased if the capillary regime of deposition is selected.

A global scheme describing the fundamental of the dip-coating process and the more recent progresses achieved by applying the conventional process in non-conventional conditions is illustrated in Fig. 1. Parts A and B at the bottom describe the driving forces and the chemical and processing parameters that govern the deposition and the final thickness. The equation (part C) links the final thickness to the solution chemical and processing conditions and is composed of 2 main terms: the rate of evaporation divided by the speed (Eu^{-1}) that describes the capillary regime of deposition (the red part of the graphic) and the solution physical chemical characteristic times the speed ($Du^{2/3}$) that describes the viscous drag regime of deposition (the blue part of the graphic). An intermediate regime, described by both intermixed regimes, is present (the green part of the graphic). Parts (D), (E) and (F) inform on which regime is preferable to choose to elaborate which systems, together with microscopic

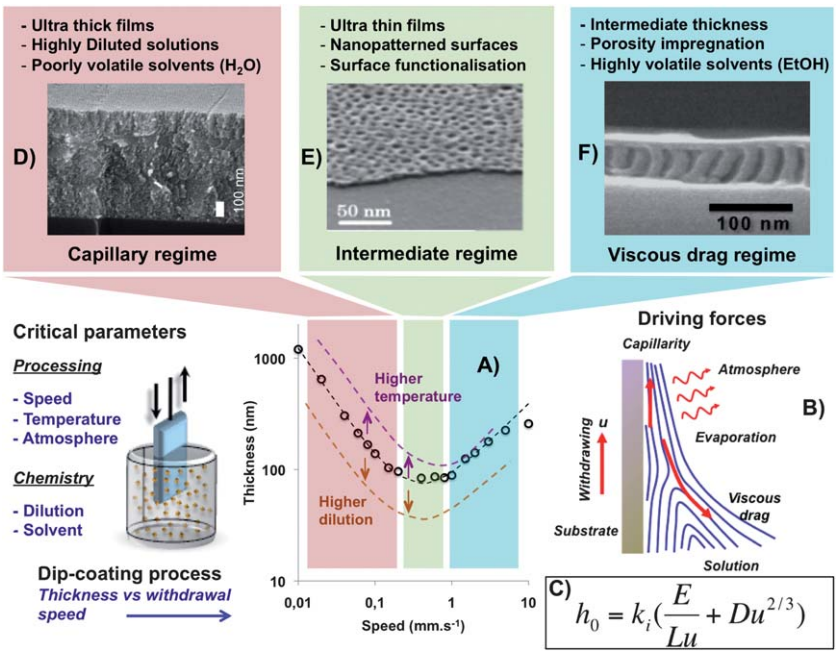

Fig. 1 Recent progresses made in the preparation of thin films by dip-coating through variation of chemical and processing conditions. (A) Typical plots of thickness *versus* withdrawal speed showing the 3 regimes of deposition (3 colors). The open rings correspond to experimental points obtained for a typical mesoporous silica film. The purple and orange curves correspond to how the latter curve would evolve upon an increase in atmospheric temperature and upon dilution of the solution, respectively. (B) Scheme of the various driving forces governing the deposition; and (C) equation describing the thickness h_0 *versus* the solution composition constant k_i, the withdrawal speed u, the evaporation rate E, the substrate width L, and the solution physical–chemical characteristics D, as described by Faustini *et al.*[8] (D) typical mesoporous TiO_2 thin film obtained in the capillary regime from aqueous solutions.[10] (E) Ultrathin nanoperforated ZrO_2 layer obtained in the intermediate regime.[11] (F) An example of a replication of a nanoporous polystyrene template by silica obtained in the viscous drag regime.[12]

images of selected typical systems. All information gathered in Fig. 1 is discussed in detail in what follows.

Dip-coating mechanism and thickness control

In the dip-coating method, the substrate is successively dipped into the solution and withdrawn at a constant speed. A layer of the non-volatile species is obtained above the drying line. Appropriate solvents are usually alcohols because they have low surface tension and are fairly volatile to promote relatively fast evaporation. The Landau–Levich model,[9] which relies on the gravity induced viscous drag opposing the adhesion of the fluid on the substrate for a Newtonian and non-evaporating fluid, is usually referred. It predicts that the equilibrium thickness depends on the density, the surface tension, and the viscosity of the fluid and is proportional to the withdrawal speed at the power 2/3.

This tendency is only verified in a narrow range of speed centered around a few mm s^{-1}. A power of 1/2 has even been reported for some SiO_2 and TiO_2 based systems and in specific conditions (solution viscosity and density, and withdrawal speed range).[13] Some works have been conducted to improve this model using simplified systems.[14–19] However, they all fail to verify the corresponding experimental tendencies because most of the dip-coated solutions are non-Newtonian as a result of their viscosity and surface tension that are continuously modified upon solvent evaporation and/or simultaneous polymerisation. While dip-coating can be used to deposit biomolecules, polymers or metallic nano-particles,[20–23] it is widely applied to perform metallic oxide coatings from sol–gel solutions.[24] Fig. 2A displays the log–log evolution of the thickness of various sol–gel-based films *versus* the withdrawal speed.[8] It clearly shows that two independent, and opposite in tendency, regimes of deposition exist at "extreme" speeds, while they counterbalance at intermediate speeds to create a minimum. Disregarding all evaporation dependent quantitative parameters and examining only the slopes, the viscous drag regime, characterised by the Landau–Levich model, was verified for speeds above 1 mm s^{-1}. Similarly, the capillary regime, where the deposition is governed by the combination of convective capillarity and evaporation effects, is found at speeds below 0.1 mm s^{-1}. The intermediate regime is thus located between 0.1 and 1 mm s^{-1}, where the minimal thickness is obtained. For all speeds, the thickness is perfectly described by the sum of the contribution of each regime, which led to the semi-experimental model (equation, Fig. 1 (C)).[8] It shows that one does not have to integrate time-dependent phenomena such as viscosity variation, evaporation cooling, and thermal Marangoni flow to predict the thickness. Ultra-low to ultra-thick films can be prepared using the same solution with a good control on the thickness. Because the capillary regime is governed by the evaporation rate E, the speed of deposition can be considerably increased using warm air. It can also be used to prepare optical quality films from aqueous solutions, since water surface tension decreases with increasing temperature. The typical evolution of the film thickness *versus* withdrawal speed with atmospheric temperature and initial solution dilution is shown in plots of Fig. 2B and C, respectively. While, modifying the dilution leads to a variation of the final thickness that is roughly similar in both regimes, increasing the atmospheric temperature induces faster deposition only in the capillary regime due to faster evaporation rate. Detailed descriptions of the tendencies can be found in ref. 8. In view of these observations, it is clear that the degree of control, involving chemical and processing parameters, is much better in dip-coating than in any other CSD processes,

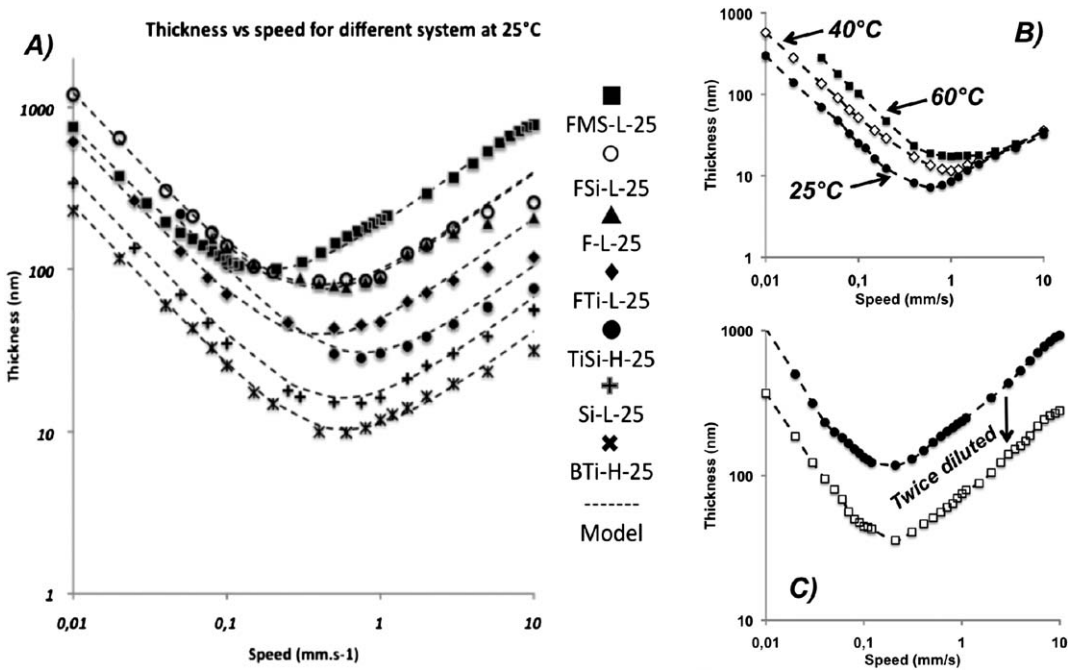

Fig. 2 (A) Evolutions of final film thickness with the withdrawal speed for various kinds of systems[8] such as mesoporous silica (FSi) and hybrid silica (FMS), polyethylene oxide-based block copolymers (F), mesoporous TiO_2 (FTi) and (Bti), dense mixed TiO_2–SiO_2 (TiSi) or pure SiO_2 (Si). (B) Typical evolutions of final film thickness with the withdrawal speed depending on the atmospheric temperature (mesoporous TiO_2 system). Typical evolutions of final film thickness with the withdrawal speed depending on the dilution (mesoporous hybrid SiO_2 system).

which makes it more attractive, versatile and accurate.

Ultra-thin (nanostructured) layers

According to the relation between the final thickness and the withdrawal speed, it is clear that the minimal thickness that can be obtained from one given solution corresponds to the intermediate specific speed when both regimes of deposition perfectly counterbalance each other. At this critical speed, reducing the thickness further down to a few nanometres necessitates the dilution of the initial solution (see Fig. 2(C)). These extreme conditions have been recently exploited to produce nanostructured Inorganic Nano Patterns (INP)[11] that are ultrathin (4–15 nm thick) metal oxide (TiO_2, Al_2O_3, and ZrO_2) layers bearing ordered nanoperforations (10–80 nm in diameter) through which the surface of the substrate (*e.g.* Si, glass, FTO, ITO, Au, or any other porous or dense layer) is accessible (see Fig. 3). Because of their thinness, they can be seen as ordered heterogeneous nanostructured surfaces. They have been utilized as substrates for selective local growth of nanoobjects such as (i) FePt nanoparticles using electrodeposition,[25] (ii) Prussian blue analogue nanoparticles using layer by layer construction,[26] (iii) CoPt nanostructured multilayer using sputtering,[27,28] or (iv) Ge nanoparticles using solid dewetting[29] for data storage systems. They have also been used as surfaces with controlled wetting properties,[30,31] as a component for antireflective self-cleaning layers,[32] or to prepare ultra-nano-electrode arrays.[33–35] Microscopy images illustrating some of these systems are given in Fig. 3.

Ultra-thick (nanostructured) layers

In the Landau–Levich regime, building ultra-thick films is limited by the gravity-induced draining, while in the capillary regime, one can indefinitely increase the thickness by reducing the withdrawal speed. However, and very often in the case of inorganic coatings, increasing the thickness of the final film is not limited by the deposition process but more by the cracks created by the lateral tensile stress induced by the densification of the layer. The solution to reduce this effect is to avoid using intermediate precursors that would create high cross-linking-induced-shrinkage after deposition. Aqueous solutions are thus ideal since they contain oxo, aquo and hydroxo precursors giving minimal shrinkage upon condensation due to the small size of the ligands. While depositing aqueous solution in the Landau–Levich regime is difficult due to the high surface tension of water, it can easily be achieved in the capillary regime.

For instance, crystalline mesoporous TiO_2 coatings have been prepared from simple $TiCl_4$, H_2O and PEO-PPO-PEO block copolymer template solutions, with thickness above 500 nm in one step,[10] which has never been achieved from classical alcoholic solutions (see Fig. 1D). This approach has also been successfully applied to prepare the first MOF films from colloidal solutions[36] of MIL-89[37] or ZIF-8,[38] as illustrated in Fig. 4. This regime is also well suited for deposition of aqueous solutions with extremely low concentrations, such as metallic colloidal solutions that are unstable at high concentrations.

Impregnation of the porosity

Coming back to the thick layers of mesoporous TiO_2, above 500 nm thickness in one step is a good performance but thicker films are often required for energy conversion and detection threshold in sensing for

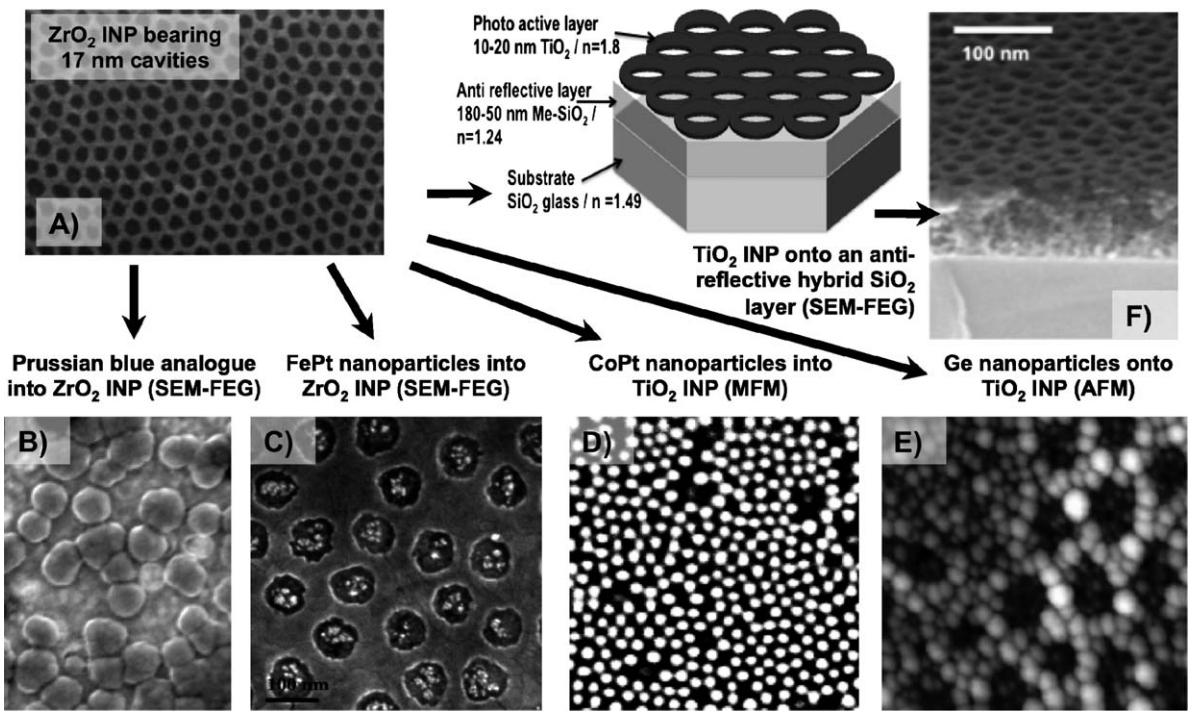

Fig. 3 (A) SEM image of a typical ZrO_2 Inorganic NanoPatterns (INP) made by dip-coating ultrathin layers of *block*-copolymers and inorganic precursors ($ZrCl_4$), and some of their utilizations as heterogeneous substrates for selective nucleation growth or as components for multilayer systems (B and C: systems obtained from ZrO_2 INP; D, E and F: systems obtained from TiO_2 INP).

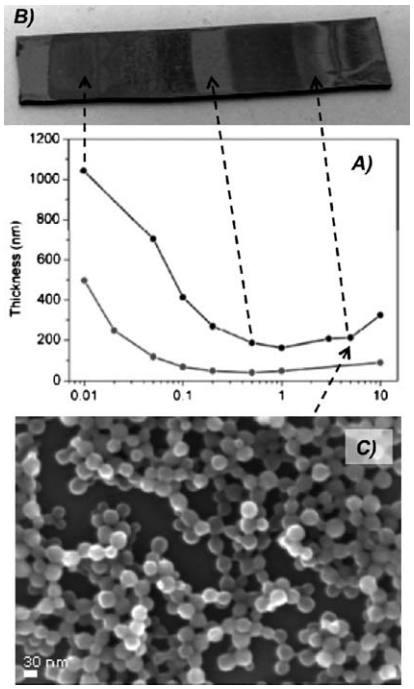

Fig. 4 (A) Effect of the withdrawal speed on the thickness obtained from an ethanolic colloidal solution of ZIF-8 with two different concentrations (0.2 mol L^{-1} up and 0.02 mol L^{-1} down) at room temperature. (B) Optical photograph of a 1×5 cm^2 sample composed of ZIF-8 nanoparticle films deposited on Si wafer. Films were obtained at 0.01 mm s^{-1} (left) to 1 mm s^{-1} (right). (C) SEM image of a typical 200 nm thick organisation of the ZIF-8 nanoparticles on the surface.

instance. The most developed method, especially used for stack heterogeneous multilayers,[39] involves several successive depositions, which is rendered delicate due to the possibility for the precursors to impregnate the porosity of the underlying layer.[40] Preventing the inorganic precursor to infiltrate the porosity is possible by filling up this latter by an organic pore-blocking agent that can be removed afterward. Such a blocking of the porosity has been achieved by liquid deposition/infiltration of F127 copolymer into 400 nm thick mesoporous TiO_2 films. Four successive deposition cycles led to the preparation of close to 2000 nm thick final mesoporous TiO_2 films, with a top porosity identical to the bottom one.[10] Due to the robustness of the protocol, the thickness can be infinitely increased if desired.

Infiltration can also be used to replicate the porous network of a template coating. The procedure involves the infiltration of precursors, the condensation within the porosity and the elimination of the initial solid template. Dip-coating is well adapted to homogeneously infiltrate networks of nanopores since air from the porosity is easily replaced by the solution due to the unidirectional progression of the linear meniscus (surface/solution/air triple line) upon withdrawing. When evaporation occurs, the constant increase of the concentration in non-volatile species induces the osmophoresis diffusion of these species into the porosity. The final step concerns evaporation from the porosity. At this point the liquid/vapour interface is defined by the pore size and a highly curved meniscus progresses from the top to the bottom of the template in each *pore*, simultaneously depositing the precursors at the surface of the porous network. An extra layer of precursor can be formed at the surface if an excess of solution was initially dip-coated. However, in some cases, several impregnation cycles are necessary to optimise the filling of the porosity. Replication of mesoporous silica films by crystalline SnO_2[41] or ZnO[42] has been reported. In these cases, only 60% of the initial porous volume could be infiltrated due to the progressive occlusion of the porosity (pore blocking) upon cycling. However, the nanostructured periodicity and symmetry have been retained after SiO_2 dissolution in KOH, and the final porosity corresponds exactly to the reverse of the initial SiO_2 template (see Fig. 5).

Infiltration by sol–gel solutions was also applied to replicate ordered nanoporous polymer layers. The initial template is obtained by liquid deposition of a block copolymer layer, such as PS-*b*-PLA or PS-*b*-PMMA, onto a substrate followed by controlled microphase separation, UV reticulation of the PS network and selective chemical etching of the counter block in alkaline solution.[3,4] The final PS template coating bears hexagonally ordered transversal cylindrical nanopores. Replication of this PS template by titano-silica compositions led to the formation of a unique nanoporous film morphology made of an array of vertical nanopillars supporting a plain layer of the same composition (the roof), as shown in Fig. 6.[12] While the dispersion, the diameter and the height of the pillars are controlled by the PS template characteristics (relative and absolute polymer block length and template thickness), the thickness of the roof is controlled by the excess amount of sol–gel solution.[12] The

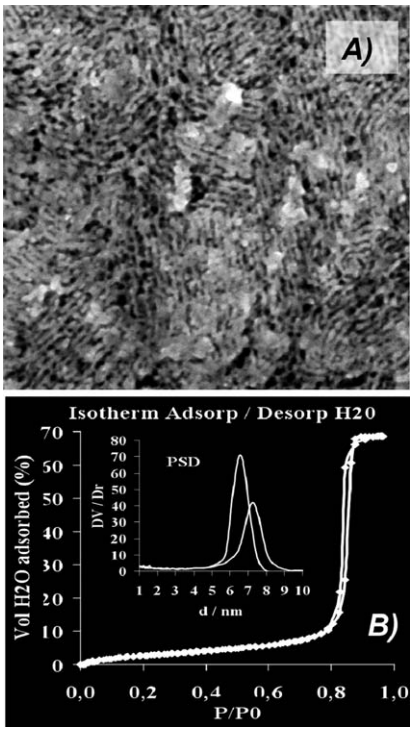

Fig. 5 (A) SEM image of the surface of a nanocrystalline ZnO mesoporous film obtained by impregnation and replication of an initial mesoporous SiO_2 template layer. (B) Corresponding water adsorption/desorption isotherm obtained by Ellipsometry Porosimetry, revealing 70% vol porosity composed of homogeneous 7 nm size pores. See ref. 42 for experimental details and interpretation.

latter morphology in Pillar Planar Nano-Channels is highly suitable for separation and analysis in nanofluidic applications. Indeed, these porous networks are highly homogeneous and free of dead-ends, making them highly suitable media to convey fluids. In addition, the inter- and intra-pillar porosities and chemical composition can be perfectly controlled by the sol–gel process. As shown in Fig. 6C, if sufficiently low amounts of sol–gel precursors are deposited, only pillars are formed, which can be useful in many domains of nanotechnology for which nanopatterned materials are required.

Conclusions

These recent progresses confirmed that dip-coating is thus much more than a simple method to prepare films onto substrates from liquid solutions. In addition to the possibility of accurately adjusting the amount of material that can be deposited, and therefore the thickness of the final film

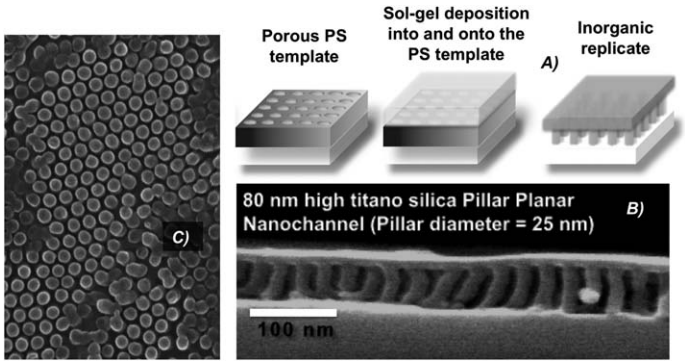

Fig. 6 (A) Preparation method of Pillar Planar Nanochannel (PPN) by replication of a nanoporous polystyrene template involving the dip-coating/infiltration by a sol–gel solution. (B) TEM image of the profile of titanosilicate PPN. (C) Pillars obtained by replication of the PS template without deposition of an excess of the solution at the surface.

(in the range of 10 to 1000 nm) using the same initial solution, the process is ideally combinable with molecular, macromolecular and nano-particular self-assembly to prepare nanostructured materials. This is due to the facile controlled modification of the wet layer composition through dynamic exchange with the atmosphere by altering the vapour pressure. Two regimes of deposition, governed either by capillary rise or viscous drag, both counterbalanced by evaporation, permit starting from virtually any kind of solution, even purely aqueous ones, and to favour either fast or slow assembly of non-volatile species onto the surface, which is impossible to achieve with spin or spray coating. Dip-coating is also highly suitable to homogeneously impregnate a porosity as a result of the progressive evaporation that tends to drag solutes within the porous network upon solvent departure. Finally, it is a low-cost, waste-free, low energy consumption, simple, easy to access, and facile to scale up technique that will with no doubt naturally self-impose even more in the coating community in the future. However, effects of many other processing parameters on the final structure and morphology of the films still need to be explored.

References

1 C. J. Brinker, A. J. Hurd, P. R. Schunk, G. C. Frye and C. S. Ashley, *J. Non-Cryst. Solids*, 1992, **147**, 424–436.
2 C. Sanchez, C. Boissiere, D. Grosso, C. Laberty and L. Nicole, *Chem. Mater.*, 2008, **20**, 682–737, Special issue.
3 D. A. Olson, L. Chen and M. A. Hillmyer, *Chem. Mater.*, 2008, **20**, 869–890.
4 H.-C. Kim, S.-M. Park and W. D. Hinsberg, *Chem. Rev.*, 2010, **110**, 146–177.
5 D. Grosso, F. Cagnol, G. J. de A. A. Soler-Illia, E. L. Crepaldi, P. A. Albouy, H. Amenitsch, A. Brunet-Bruneau and C. Sanchez, *Adv. Funct. Mater.*, 2004, **14**, 309–322.
6 H. Kozuka, *J. Sol-Gel Sci. Technol.*, 2006, **40**, 287–297.
7 T. Kurisu and H. Kozuka, *J. Am. Ceram. Soc.*, 2006, **89**, 2453–2458.
8 M. Faustini, B. Louis, P. A. Albouy, M. Kuemmel and D. Grosso, *J. Phys. Chem. C*, 2010, **114**, 7637–7645.
9 L. Landau and B. Levich, *Acta Physicochim. URSS*, 1942, **17**, 42–54.
10 N. Krins, M. Faustini, B. Louis and D. Grosso, *Chem. Mater.*, 2010, **22**, 6218–6220.
11 M. Kuemmel, J. Allouche, L. Nicole, C. Boissière, C. Laberty, H. Amenitsch, C. Sanchez and D. Grosso, *Chem. Mater.*, 2007, **19**, 3717–3725.
12 M. Faustini, M. Vayer, B. Marmiroli, M. Hillmyer, H. Amenitsch, C. Sinturel and D. Grosso, *Chem. Mater.*, 2010, **22**, 5687–5694.
13 M. Guglielmi, P. Colombo, F. Peron and L. M. D. Esposti, *J. Mater. Sci.*, 1992, **27**, 5052–5056.
14 C. Y. Lee and J. A. Tallmadge, *Ind. Eng. Chem. Fundam.*, 1976, **15**, 258–266.
15 R. P. Spiers, C. V. Subbaraman and W. L. Wilkinson, *Chem. Eng. Sci.*, 1974, **29**, 389–396.
16 B. G. Higgins, W. J. Silliman, R. A. Brown and L. E. Scriven, *Ind. Eng. Chem. Fundam.*, 1977, **16**, 393–401.
17 P. R. Schunk, A. J. Hurd and C. J. Brinker. *Liquid Film Coating*, Chapman & Hall, London, 1997, pp. 673–708.
18 A. V. Kuznetsov and M. Xiong, *Int. Commun. Heat Mass Transfer*, 2002, **29**, 35–44.
19 C. H. Lee, Y. F. Lu and A. Q. Shen, *Phys. Fluids*, 2006, **18**, 052105.
20 M. Le Berre, Y. Chen and D. Baigl, *Langmuir*, 2009, **25**, 2554–2557.
21 J. Conway, H. Korns and M. R. Fisch, *Langmuir*, 1997, **13**, 426–431.
22 T. Kraus, L. Malaquin, H. Schmid, W. Riess, N. D. Spencer and H. Wolf, *Nat. Nanotechnol.*, 2007, **2**, 570–576.
23 E. Rabani, D. R. Reichman, P. L. Geissler and L. E. Bruss, *Nature*, 2003, **426**, 271–274.
24 C. J. Brinker, G. C. Frye, A. J. Hurd and C. S. Ashley, *Thin Solid Films*, 1991, **201**, 97–108.
25 J. Allouche, D. Lantiat, M. Kuemmel, M. Faustini, C. Laberty, C. Chaneac, E. Tronc, C. Boissiére, L. Nicole, C. Sanchez and D. Grosso, *J. Sol-Gel Sci. Technol.*, 2010, **53**, 551–555.
26 S. Lepoutre, D. Grosso, C. Sanchez, G. Fornasieri, E. Riviere and A. Bleuzen, *Adv. Mater.*, 2010, **22**, 3992–3996.
27 D. Makarov, P. Krone, D. Lantiat, C. Schulze, A. Liebig, C. Brombacher, M. Hietschold, S. Hermann, C. Laberty, D. Grosso and M. Albrecht, *IEEE Trans. Magn.*, 2009, **45**, 3515–3518.
28 C. Schulze, M. Faustini, J. Lee, H. Schletter, M. U. Lutz, P. Krone, M. Gass, K. Sader, A. L. Bleloch, M. Hietschold, M. Fuger, D. Suess, J. Fidler, U. Wolff, V. Neu, D. Grosso, D. Makarov and M. Albrecht, *Nanotechnology*, 2010, 21, Article number 495701.
29 D. J. Lockwood, N. L. Rowell, I. Berbezier, G. Amiard, A. Ronda, M. Faustini and D. Grosso, *J. Electrochem. Soc.*, 2010, **157**, 1160–1164.
30 M. Järn, F. J. Brieler, M. Kuemmel, D. Grosso and M. Lindén, *Chem. Mater.*, 2008, **20**, 1476–1483.
31 M. Jarn, Q. A. Xu and M. Linden, *Langmuir*, 2010, **26**, 11330–11336.
32 M. Faustini, L. Nicole, C. Boissire, P. Innocenzi, C. Sanchez and D. Grosso, *Chem. Mater.*, 2010, **22**, 4406–4413.
33 C. Laberty-Robert, M. Kuemmel, J. Allouche, C. Boissière, L. Nicole, D. Grosso and C. Sanchez, *J. Mater. Chem.*, 2008, **18**, 1216–1221.
34 D. Lantiat, V. Vivier, C. Laberty-Robert, D. Grosso and C. Sanchez, *ChemPhysChem*, 2010, **11**, 1971–1977.
35 M. Faustini, B. Marmiroli, L. Malfatti, B. Luois, N. Krins, P. Falcaro, G. Grenci, C. Laberty-Robert, H. Amenitsch, P. Innocenzi and D. Grosso, *J. Mater. Chem.*, 2011, **21**, 3597–3603.
36 P. Horcajada, C. Serre, D. Grosso, C. Boissiere, S. Perruchas, C. Sanchez and G. Ferey, *Adv. Mater.*, 2009, **21**, 1931–1935.
37 A. Demessence, P. Horcajada, C. Serre, C. Boissiere, D. Grosso, C. Sanchez and G. Ferey, *Chem. Commun.*, 2009, 7149–7151.
38 A. Demessence, C. Boissiere, D. Grosso, P. Horcajada, C. Serre, G. Ferey, G. J. A. A. Soler-Illia and C. Sanchez, *J. Mater. Chem.*, 2010, **20**, 7676–7681.
39 M. C. Fuertes, S. Colodrero, G. Lozano, A. R. Gonzales-Elipe, D. Grosso, C. Boissiere, C. Sanchez, G. J. A. A. Soler-Illia and H. Miguez, *J. Phys. Chem. C*, 2008, **112**, 3157–3163.
40 J. Dewalque, R. Cloots, F. Mathis, O. Dubreuil, N. Krins and C. Henrist, *J. Mater. Chem.*, 2011, **21**, 7356–7363.
41 S. Lepoutre, J. H. Smatt, C. Laberty, H. Amenitch, D. Grosso and M. Linden, *Microporous Mesoporous Mater.*, 2009, **123**, 185–192.
42 S. Lepoutre, B. Julián-López, C. Sanchez, H. Amenitsch, M. Linden and D. Grosso, *J. Mater. Chem.*, 2010, **20**, 537–542.

